Environmental
Science
Processes & Impacts

ROYAL SOCIETY
OF CHEMISTRY
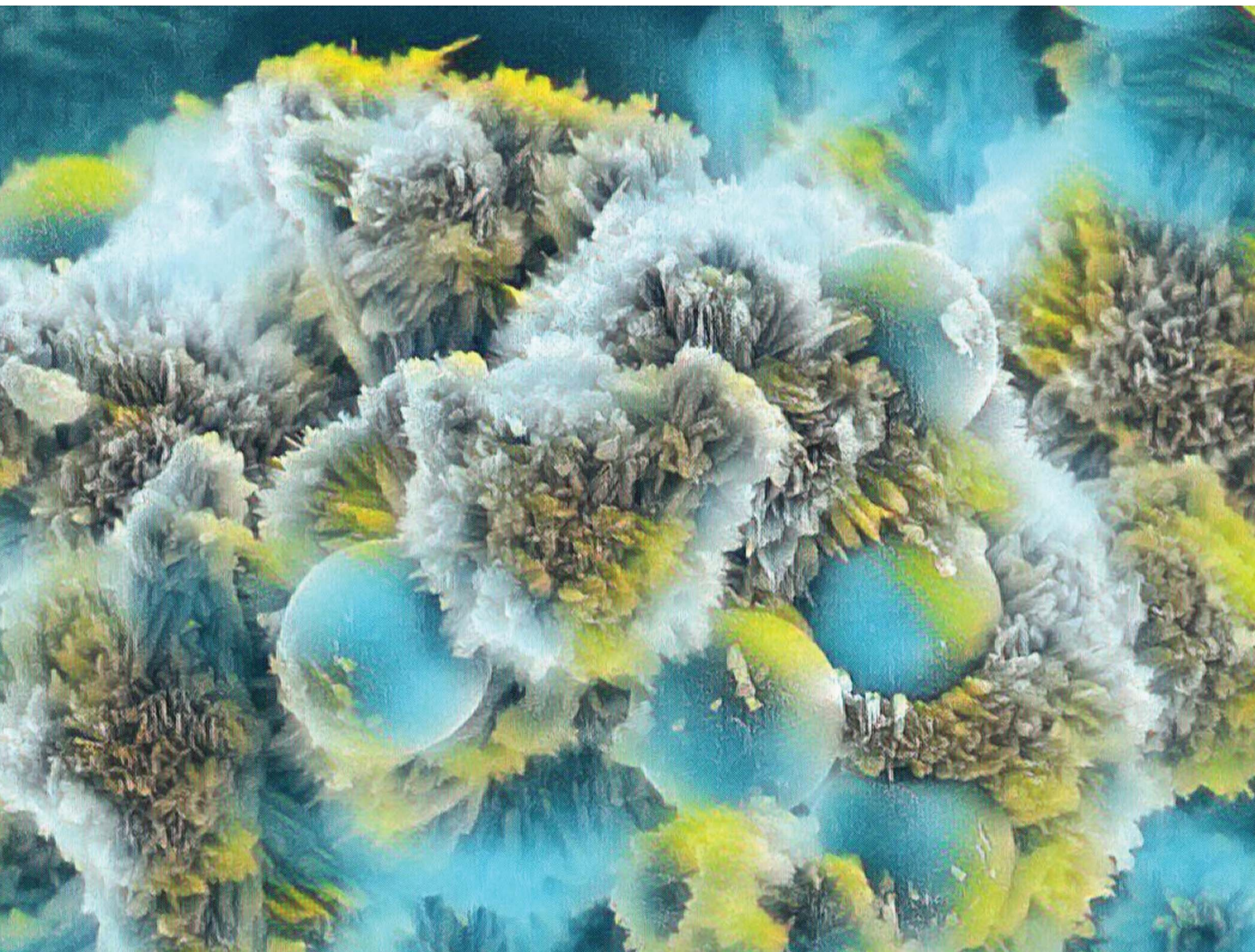
PAPER
J. Kontrec, N. Matijaković Mlinarić, B. Njegić Džakula *et al.*
Microplastics encapsulation in aragonite: efficiency,
detection and insight into potential environmental impacts

PAPER

Check for updates

Microplastics encapsulation in aragonite: efficiency, detection and insight into potential environmental impacts†

Nives Matijaković Mlinarić, [ID] [a] Katarina Marušić,[a] Antun Lovro Brkić, [ID] [b] Marijan Marciuš,[a] Tamara Aleksandrov Fabijanić,[d] Nenad Tomašić,[c] Atiđa Selmani, [ID] [e] Eva Roblegg,[e] Damir Kralj,[a] Ivana Stanić, [ID] [a] Branka Njegić Džakula [ID] *[a] and Jasminka Kontrec [ID] *[a]

Plastic pollution in aquatic ecosystems has become a significant problem especially microplastics which can encapsulate into the skeletons of organisms that produce calcium carbonates, such as foraminifera, molluscs and corals. The encapsulation of microplastics into precipitated aragonite, which in nature builds the coral skeleton, has not yet been studied. It is also not known how the dissolved organic matter, to which microplastics are constantly exposed in aquatic ecosystems, affects the encapsulation of microplastics into aragonite and how such microplastics affect the mechanical properties of aragonite. We performed aragonite precipitation experiments in artificial seawater in the presence of polystyrene (PS) and polyethylene (PE) microspheres, untreated and treated with humic acid (HA). The results showed that the efficiency of encapsulating PE and PE-HA microspheres in aragonite was higher than that for PS and PS-HA microspheres. The mechanical properties of resulting aragonite changed after the encapsulation of microplastic particles. A decrease in the hardness and indentation modulus of the aragonite samples was observed, and the most substantial effect occurred in the case of PE-HA microspheres encapsulation. These findings raise concerns about possible changes in the mechanical properties of the exoskeleton and endoskeleton of calcifying marine organisms such as corals and molluscs due to the incorporation of pristine microplastics and microplastics exposed to dissolved organic matter.

Environmental significance

Improper disposal of plastic waste leads to its accumulation in aquatic ecosystems. Microplastic particles are particularly hazardous to smaller organisms such as molluscs and corals. The encapsulation of microplastics into precipitated aragonite, the main inorganic component of coral skeleton, has not been previously studied. In this study, we investigated the encapsulation of polyethylene and polystyrene microplastic particles, untreated and treated with humic acid, into precipitated aragonite. The results showed that microplastic particles were encapsulated into aragonite, and consequently changed aragonite properties. The encapsulation of humic acid-treated polyethylene microspheres yielded the most significant impact on aragonite mechanical properties. Our findings raise concerns about potential changes in coral skeletal tissue due to the encapsulation of various microplastics.

1. Introduction

Calcium carbonate minerals are widely distributed in various aquatic ecosystems.[1] Marine organisms use $CaCO_3$ for many purposes such as mechanical reinforcement (formation of defensive shells, teeth, bones), optical filtering, and focusing. In marine invertebrate organisms, the mineralised tissues (exoskeleton and endoskeleton) are most commonly built of calcite, the most stable modification of calcium carbonate or aragonite, while vaterite is rarely found. Aragonite is a high-temperature modification, but is well known for precipitating in marine and terrestrial media.[2,3] The nucleation and growth of aragonite *versus* calcite in the marine environment have been

[a]*Division of Materials Chemistry, Ruđer Bošković Institute, Bijenička cesta 54, 10000 Zagreb, Croatia. E-mail: jasminka.kontrec@irb.hr; bnjeg@irb.hr; Tel: +385 1 456 1004*

[b]*Institute of Physics, Bijenička cesta 46, 10000 Zagreb, Croatia*

[c]*Department of Geology, Faculty of Science, University of Zagreb, Horvatovac 102a, Zagreb, Croatia*

[d]*The Faculty of Mechanical Engineering and Naval Architecture, University of Zagreb, Ivana Lučića 5, 10000 Zagreb, Croatia*

[e]*Pharmaceutical Technology and Biopharmacy, Institute of Pharmaceutical Sciences, University of Graz, Universitätsplatz 1, 8010 Graz, Austria*

1116 | *Environ. Sci.: Processes Impacts*, 2024, **26**, 1116–1129

This journal is © The Royal Society of Chemistry 2024

attributed to various factors, such as pH, Mg/Ca ratio, pCO_2, supersaturation, and inhibitors.[4,5] However, reaction mechanisms and environmental controls are still not fully understood. Mg^{2+} ions are well-known to promote aragonite over calcite nucleation and crystal growth. Among others, corals are organisms whose skeleton is built from calcium carbonate. In these organisms, the mineralized tissues are built from calcium carbonate polymorph – aragonite.[1] Coral reefs cover approximately 250 000 km^2 of seafloor worldwide, and these complex systems provide habitat for more than 500 000 species.[6] For humans, they provide food and resource security, coastal protection, ocean recreation, tourism and coastal livelihoods, socio-cultural services, and biogeochemical cycling.[7] Such ecosystems are among the most biologically rich and productive ecosystems on Earth. However, unfortunately, climate change has left them vulnerable to pollution, temperature increases that lead to coral bleaching, and ocean acidification that reduces their growth.[8]

Plastic pollution is in the spotlight as millions of tons of plastic waste are disposed into aquatic ecosystems yearly.[9] Over time and under the influence of UV irradiation, mechanical breaking, and the impact of microorganisms, bigger plastic pieces break down into smaller micro and nanoparticles.[10] About 400 million tonnes of plastic waste is global annual production and this quantity is expected to increase over the coming decades.[11,12] Estimated between 60 and 99 million metric tonnes (Mt) of mismanaged plastic waste (MPW) were produced globally in 2015 and most of it being discarded into landfill or released into the natural environment. It is estimated that about 8 million metric tons (Mt) of macroplastic[13] and 1.5 Mt of primary microplastic[14] enter the ocean annually. A recent report by the UN Environment Programme[15] estimated over 10 million Mt of plastic enter aquatic ecosystems annually. According to one estimate, the world is on track to accumulate roughly 12 billion tonnes of plastic waste in landfills and the natural environment by 2050.[16] Analysis by Lau et al.[17] shows that implementing all feasible interventions could reduce plastic pollution by 40% from 2016 rates and 78% relative to "business as usual" in 2040. Even with immediate and concerted action, 710 million metric tons of plastic waste will cumulatively enter aquatic and terrestrial ecosystems. So, our progress to reduce plastic pollution has been painfully slow and the consequent damage to the natural environment and human health is likely to increase further.[18]

Microplastic particles are particularly hazardous to smaller animals such as foraminifera, molluscs, and corals because they get embedded in their skeletons and soft tissues.[19–22] Direct contact of corals with microplastics can lead to tissue necrosis and microplastic overgrowth of coral tissue and skeleton.[20,21,23–25] Microplastics permanently accumulate in coral reefs as living biological sinks, with a small number of particles entrapped in coral soft tissue (up to 2 particles per cm^2) and a much higher number entrapped in the skeleton (up to 84 particles per cm^3).[26] The encapsulation of microplastics in the coral skeleton is of concern because it can accumulate over time as the coral skeleton continuously grows and the microplastics are constantly present.

To date, only a few studies have reported the effect of plastic particles on the precipitation of calcium carbonate, namely calcite. Experimental studies have shown that nano and microscale plastic particles of polymethyl methacrylate can induce calcite nucleation with preferential binding of plastic particles to the surface of calcite crystals.[27] In addition, the encapsulation of polystyrene particles in calcite crystals occurred when the particle surface was functionalized with acrylic and fumaric acids.[28] In contrast, non-functionalized polystyrene did not cause the same effect, suggesting that the functional groups on the plastic surface significantly impact encapsulation.[28,29]

The encapsulation of microplastics into precipitated aragonite, which builds the coral skeleton, has not been studied previously. The aim of this study was to investigate the encapsulation of polyethylene (PE) and polystyrene (PS) microplastic particles into precipitated aragonite crystals in an artificial seawater precipitation system. Among the different types of plastics, PE and PS are the most abundant plastics used in consumer products and have shorter lifetimes than other plastics.[30–32] They are also among the most abundant plastics in water environments,[33,34] making them a suitable model for studying the environmental impact of plastic pollution. Studies to detect these plastic materials in the environment require more powerful diagnostic tools to identify, classify, and accurately quantify them.[35] There are a few methods used for the characterization or quantification of microplastics in a water environment: spectroscopy (μ-FTIR and Raman),[36,37] pyrolysis-gas chromatography/mass spectrometry (PyGC/MS),[38] and thermogravimetric analysis (TGA-GC/MS).[39] Recently, Total Organic Carbon analysis (TOC) of plastic particles was presented as an alternative to conventional spectroscopic and thermogravimetric methods to estimate the mass of microplastics in sewage.[40]

Microplastic particles in aquatic ecosystems get exposed to different environmental conditions like temperature, pH, and dissolved organic matter, which can change the surface of plastic particles.[41] Also, environmental factors such as UV radiation, thermo-oxidative processes, mechanical forces, chemicals and microorganisms influence changes in surface properties and plastic degradation.[42–46] Microplastic surface properties, such as roughness, area, charge, chemical functionality, hydrophobicity/hydrophilicity, colour, and appearance of cracks affect the reactivity and potential toxicity of microplastics.[47,48] There is evidence that changes in the surface properties of microplastics may affect the adsorption of chemical contaminants, surface oxidation, interactions with natural colloids and the presence of microbial biofilms.[49–51]

Dissolved organic matter is a complex mixture of amino acids, peptides, proteins, polysaccharides, and humic substances.[52] Adsorption of humic acid (HA), the reactive fraction of dissolved organic matter, can alter the environmental behaviour of microplastics.[53] Dissolved organic matter, metal cations, and microplastic particles can aggregate due to electrostatic attraction and be transported into the sediment, where organisms such as corals can reside, which is particularly

This journal is © The Royal Society of Chemistry 2024

Environ. Sci.: Processes Impacts, 2024, **26**, 1116–1129 | 1117

dangerous because such aggregates preferentially adsorb to minerals.[54–59]

Our previous study showed that organic matter, namely HA as a reactive fraction of dissolved matter, enhances the encapsulation of polystyrene microspheres in calcite crystals.[29] The present study used PE and PS microspheres as model microplastic particles and HA as the reactive fraction of dissolved organic matter to estimate microplastic encapsulation into aragonite. TOC analysis has been applied as a potential method for quantifying encapsulation efficiency. Before this analytical method is applied, pre-treatment steps for isolating encapsulated microspheres from inorganic/microplastic solid matrix are required.

We aimed to present and discuss data on preparing and characterizing aragonite in the presence of microplastics and on encapsulated microplastics analysis. Our results may indicate a problem related to possible changes in skeletal formation in corals worldwide due to the encapsulation of different microplastics.

2. Experimental

To study the encapsulation of microplastics into aragonite, experiments of calcium carbonate precipitation in artificial seawater in the presence of PS and PE microspheres, treated or untreated with HA, were performed. At that, HA was a model molecule representing the reactive fraction of dissolved organic matter ubiquitous in aquatic ecosystems. Selected types of microplastic particles were chosen because they are among the most abundant plastics in water environments.[33,34]

2.1. Materials

Analytical grade chemicals were used for precipitation experiments: sodium carbonate (Na_2CO_3, Sigma-Aldrich), potassium chloride (KCl, Kemika), sodium chloride (NaCl, Alpha Aesar), sodium sulfate (Na_2SO_4, Kemika), calcium chloride ($CaCl_2 \cdot 2H_2O$, Acros Organics), magnesium chloride ($MgCl_2 \cdot 6H_2O$, Kemika), polystyrene microspheres, PS (size 1.6 ± 0.2 μm, density 1.05 g cm^{-3}, Tianjin Baseline Chromtech Research Centre), polyethylene microspheres, PE (size 0.74–4.99 μm, density 0.98 g cm^{-3}, Cospheric LLC) and deionized water (conductivity < 0.055 μS cm^{-1}).

2.2. Precipitation experiments

Precipitation experiments were performed in a solution that mimicked artificial seawater (ASW) or extrapallial solution of marine and freshwater species[60] and had the composition: presented in Table SI1.† Initial supersaturation, as one of the critical parameters controlling the precipitation of $CaCO_3$, was identical in all the systems. It is expressed as the saturation ratio with respect to aragonite, S_A (definition in the ESI† in the paragraph titled "Calcium carbonate precipitation") and was set to 8.5. Two reactant solutions were prepared: A and B. Half of the total amount of sodium chloride was added to each solution A and B, which were prepared by dissolving $CaCl_2$, $MgCl_2$, and KCl and by dissolving Na_2CO_3 and Na_2SO_4, respectively. Total ion concentrations in artificial seawater (Table SI1†) were obtained by mixing equal volumes (200 cm^3) of reactant solutions A and B in a thermostated (298 K) double-walled glass vessel under constant stirring with a Teflon-coated magnetic stirring bar. The untreated or humic acid-treated microspheres were added to solution B before mixing the two reactant solutions. Experiments were initiated by fast mixing of solution A into solution B. The progress of precipitation was followed by measuring pH *versus* time (pH/ion meter, Radiometer PHM 240). After two hours of precipitation, an additional 60 mL of each solution (A and B) was added dropwise at 0.5 mL min^{-1} to achieve a high product yield. Each experiment was repeated three times. After one hour, the suspensions were filtered through a membrane filter (0.22 μm), and the precipitate was dried at 50 °C for two hours.

2.3. Preparation of plastic microspheres with humic acid

The HA-treated plastic microspheres (PS-HA and PE-HA) were prepared as previously described.[29] PS or PE microspheres (8 mg) were rotated in 300 μL of HA solution (4000 mg dm^{-3}) for 30 minutes, centrifuged, and washed with deionized water in three cycles. Since one of the objectives of this study was to determine the general effect of humic acid on the encapsulation of microplastic particles in calcium carbonate, a much higher concentration of humic acid than that observed in seawater was used as explained in Matijaković Mlinarić *et al.*[29] The short time of incubation of microplastics (30 min) in high concentrations of humic acid (4000 mg L^{-1}) was performed to accelerate the ageing of microplastics under the influence of dissolved organic matter and, in that way, to simulate the change in surface characteristics of microplastic, namely roughness, and wettability. In addition, before initiating aragonite precipitation experiments, the microparticles were thoroughly washed in several cycles with water to eliminate any free or non-adsorbed humic acid molecules that could influence the growth of aragonite crystals.

2.4. Characterization

The surface properties of the untreated and HA-treated microspheres were determined by atomic force microscopy (AFM) in AC mode using NanoWizard 4 ULTRA AFM (Bruker) as previously described.[29] During AFM imaging topography, amplitude and phase images were acquired simultaneously. Multi75Al-G AFM probes (BudgetSensors) were used. The freshly exfoliated HOPG substrate was covered with 1 μL of the prepared solution (γ(microspheres) = 11 g dm^{-3}) and dried on a hot plate set to 60 °C. The obtained images were processed using JPKSPM data processing software, while Gwyddion software[61] was used to determine RMS surface roughness. Due to the sphere curvature, the processing was conducted on the smaller-scale images using a fourth-order polynomial fit.

Contact angle and colourimetric measurements were performed on pellets with 5 mm diameter prepared by pressing 15 mg of untreated and HA-treated PE and PS microspheres in a hydraulic press with 2 tonnes for 2 min. Untreated samples were pure PE and PS chemicals, while HA-treated PE and PS

1118 | *Environ. Sci.: Processes Impacts*, 2024, **26**, 1116–1129

This journal is © The Royal Society of Chemistry 2024

were prepared as follows: 50 mg of microspheres (PS and PE) were rotated for 30 minutes in 10 mL of artificial seawater (ASW) with the addition of 0.1 mL 4000 ppm humic acid, filtered through a membrane filter (0.22 µm) washed with deionized water and dried at room temperature. Three measurements were performed on each sample type, and the calculated mean values are presented in the manuscript. Wettability of the PE and PS pellets was assessed by solid–liquid contact angle (θ) measurements performed with a goniometer (DataPhysics, OCA 25, Germany), dropping 1 µL of deionized water and capturing droplet snapshots immediately after release from the syringe (within ~0.5 s). A Konica Minolta® spectrophotometer model CM-2600d was used to measure the colour of the samples. A detailed description of the method is given in ESI† (in the paragraph titled "Contact angle and colour measurements"). The specific surface area of microplastics was determined by the (Brunnauer–Emmet–Teller) BET technique with N_2 adsorption using the Gemini 2380 instrument (Micromeritics, USA). Electrophoretic light scattering Nano ZS was used to determine the zeta potential of microplastics (ELS, Malvern Instruments, Malvern, United Kingdom). Dry samples were dispersed in saturated $CaCO_3$ solution (filtered through Whatman filters with a pore size of 0.45 µm) and sonicated for 15 min, followed by zeta potential measurements. All measurements were performed in triplicate at 25 °C.

The composition of the prepared samples was analysed by Fourier-transformed infrared spectroscopy and X-ray powder diffraction. Potassium bromide pellets were prepared, and the infrared spectra were recorded in the 400–4000 cm^{-1} region, using 16 scans and 2 cm^{-1} resolution on TENSOR II (Bruker). X-ray powder diffractograms have been collected on the Philips X'Pert PRO PW 3050/60 diffractometer. During the measurement, CuK$_\alpha$ source was used, and the sample diffractograms were collected in the scan range $20° \leq 2\theta \leq 60°$ (128.27 s per step, step size $2\theta = 0.026°$). The morphology of the $CaCO_3$ samples was determined using JEOL JSM-7000F (Jeol Ltd) without coating. Complete micromechanical characterization of pure aragonite (from the reference experiment) and samples with encapsulated microspheres (from experiments in the presence of PS-HA or PE-HA after isolation and dissolution of unembedded microspheres) was performed by an instrumented indentation test (IIT) using the Micro Combi Tester MCT^3 (Anton Paar). Measurements were performed on 5 mm diameter pellets prepared by pressing 40 mg of aragonite or aragonite with PS-HA and PE-HA in a hydraulic press with 2 tonnes for 2 min. A Vickers diamond pyramid was used as the indenter. Mechanical properties were evaluated using a force of 1000 mN in linear loading mode at room temperature according to EN ISO 14577-1:2015. Ten measurements were performed on each sample. The hardness and indentation modulus values were calculated using the Olivier and Pharr method with a supposed Poisson ratio of 0.3. A detailed description of the method is given in the ESI.†

2.5. Encapsulation efficiency

The amount of encapsulated PS and PE microspheres in the calcium carbonate samples was evaluated using total organic carbon analysis (TOC analysis, Elementar). The samples for total organic carbon measurements were prepared by first dissolving both the partially encapsulated/adsorbed and free microspheres (microspheres in the obtained samples that the $CaCO_3$ did not encapsulate and that can get in contact with the used organic solvents). The partially encapsulated/adsorbed and free microspheres were dissolved in chloroform (for PS or PS-HA) or in hot, boiling, xylene (for PE or PE-HA). Then, all samples were washed with acetone in 5 cycles and centrifuged (4000 rpm) for 15 min after each cycle. In the last cycle, the samples were washed with water, centrifuged, and dried at 70 °C for three hours to evaporate the remaining acetone and water. All partially encapsulated/adsorbed and free microspheres were dissolved during this process, and only the encapsulated ones remained in the sample since calcium carbonate does not dissolve in chloroform or xylene. Upon drying, the prepared samples were dissolved with hydrochloric acid (c(HCl) = 0.6 mol dm^{-3}). Hydrochloric acid dissolved calcium carbonate leaving only plastic microspheres (that were encapsulated in calcium carbonate) in the formed suspension. Then, this microsphere suspension was used for TOC analysis by burning 800 µL of the suspension, in triplicates, at 850 °C.

3. Results and discussion

3.1. Calcium carbonate precipitated in the presence of plastic microspheres

In order to closely mimic the inorganic environment of the *in vivo* formation of calcium carbonate in seawater, the precipitation of calcium carbonate in artificial seawater (Table SI1†) was used as a model system. This model system is suitable for preparing aragonite, the primary mineral component of coral skeleton.

The composition of the samples prepared in artificial seawater with or without plastic microspheres was determined by FTIR spectroscopy (Fig. 1) and XRD analysis (Fig. 2). In all precipitated samples (Fig. 1; black, red, and green lines) carbonate group vibrations of aragonite were observed: antisymmetric stretching (ν_3, C–O doubly degenerate) at 1484 and 1444 cm^{-1}, symmetric stretching (ν_1, nondegenerate) at 1083 cm^{-1}, out-of-plane bending (ν_2, CO_3 nondegenerate) at 856 cm^{-1} and in-plane bending (ν_4, O–C–O doubly degenerate) at 713 and 700 cm^{-1}.[62] The formation of aragonite is preferentially compared to other calcium carbonate polymorphs because Mg^{2+} inhibits calcite and favours aragonite nucleation.[63–66]

In addition to carbonate vibrations, groups of vibrations specific to PS and PE are visible in the aragonite samples prepared with HA-treated or untreated plastic microspheres. The infrared spectra of untreated and HA-treated commercial plastic microspheres (Fig. 1, blue lines) show specific vibration groups. The PS microspheres (Fig. 1a, blue line) show specific aromatic C–H stretching at 3066 and 3029 cm^{-1}, CH_2 stretching at 2929 and 2856 cm^{-1}, aromatic C=C stretching in the benzene ring at 1596, 1491, and 1454 cm^{-1} and out of plane C–H bending of one substituent on the benzene ring at 750 and 696 cm^{-1} which is in accordance with literature data.[67] The PE

Fig. 1 Representative infrared spectra of samples from precipitation experiments with (a) PS microspheres and (b) PE microspheres. The representative spectra are indicated for: the untreated and HA-treated microspheres (no significant difference was observed in their spectra, so only one representative spectrum is presented, blue line), pure HA (orange line), calcium carbonate precipitates obtained in the reference system (black line), calcium carbonate precipitates obtained with untreated (red line) or HA-treated microspheres (green line). The insets show a specific wavenumber range. The noted specific groups and bond vibrations show the major functional groups present in the samples.
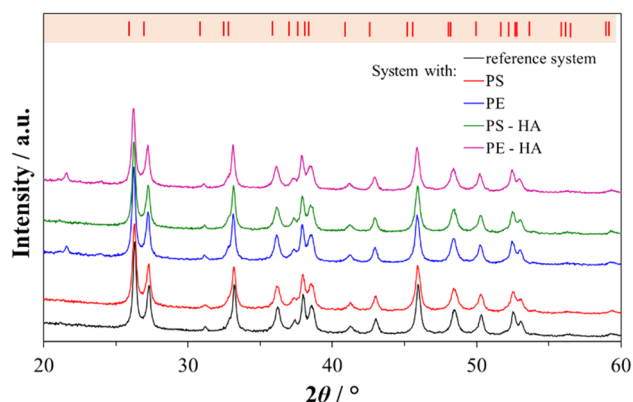

Fig. 2 X-ray diffractograms of calcium carbonate samples precipitated in the reference system and with the addition of untreated and HA-treated PS and PE microspheres. The standard diffraction line positions of aragonite (red bars) are shown for comparison.

microspheres (Fig. 1c, blue line) showed asymmetric and symmetric CH_2 stretching at 2919, 2909, 2844, 2854 cm^{-1}, C–CH_3 umbrella mode symmetric bent at 1474 and 1466 cm^{-1} and a C–CH_2 rocking at 727 and 717 cm^{-1}, as a result of close packing of methylene chains specific to high-density PE.[68]

The microspheres were treated with HA to determine the influence of organic matter on encapsulation efficiency. The spectra of pure HA (Fig. 1, orange lines) showed different functional groups: OH stretching at 3693 cm^{-1}, asymmetric and symmetric COO^- stretching at 1580 and 1383 cm^{-1}, respectively, and C–O–C stretching in the 1010–1033 cm^{-1} region.[69,70] After HA treatment of PS and PE microspheres, the adsorbed molecules were too low for spectral bands observation. To confirm the adsorption of HA, the AFM, contact angle analysis, and measurements of colour change were performed (Subsection 3.2).

The results of the XRD analysis (Fig. 2) were in good agreement with FTIR spectroscopy. The most prominent peaks were detected at 26.2°, 27.2°, 33.2°, 37.9°, 38.4°, 45.8°, 50.2° and 52.5° corresponding to (111), (021), (012), (112), (130), (221), (132) and (113) diffraction lines of aragonite (JCPDS card no. 41-1475). In the XRD diffractions of aragonite precipitated in the presence of untreated and HA-treated PE microspheres, an additional peak was observed at 21.7° 2θ, which is expected due to the presence of crystallized methylene chain regions in high-density PE.[71] The aragonite unit cell parameters did not change, which shows that the microplastic particles did not cause crystal unit distortions and indicates that the microspheres are encapsulated in aragonite without the noticeable incorporation into the crystal unit cell. Similar to the studies performed on the calcite polymorph with PS, gold, and iron microparticles, no influence on the crystal unit was observed.[29,72,73] In contrast, the incorporation of molecules and ions into the crystal unit cell can cause a change in the unit cell parameters,[74,75] which was not observed in our case.

3.2. Characterization of plastic microspheres

AFM was performed to determine the surface properties of untreated and HA-treated plastic microspheres. A large-scale image of untreated PE microspheres is shown in Fig. 3a. Further processing was conducted on the smaller-scale images, and a fourth-order polynomial fit was used to remove the sphere's curvature. The obtained images of the surface features are shown in Fig. 3b and c for untreated and HA-treated sphere surfaces, respectively. Analysis of the AFM measurements shows a higher RMS surface roughness of the HA-treated sample (80.4 ± 48.8 nm) than that of the untreated sample (8.8 ± 3.1 nm).

The difference in surface features can also be seen in the profiles of the surfaces, as shown in Fig. 3d, where the profiles correspond to the lines indicated in Fig. 3b and c. The final results clearly show that, when compared, the treated samples have higher surface roughness and distinct high features not expressed in the untreated samples.

In our previous study, the RMS surface roughness of PS microspheres was 0.9 ± 0.2 nm.[29] Compared to PE

1120 | *Environ. Sci.: Processes Impacts*, 2024, **26**, 1116–1129

This journal is © The Royal Society of Chemistry 2024

Fig. 3 AFM measurement of PE microspheres. (a) Large-scale topography image of untreated microspheres. Small-scale topography image of surface features: (b) untreated and (c) treated microspheres. (d) Profiles of untreated and treated PE surfaces (indicated with blue and green lines in (b) and (c)).

microspheres, the surface of PS microspheres is more regular, with about ten times the lower value of RMS surface roughness. After treatment of PS with HA, it increases to 1.40 ± 0.03 nm. For PE microspheres, the same treatment leads to about ten times higher RMS surface roughness. Previously, HA coating on the PS microspheres was shown to increase the microsphere size.[41] Also, it was found that HA changed the physical and chemical surface properties of polypropylene[76] and PE marine debris.[77]

Wettability and colour measurements were conducted to confirm HA adsorption on the PS and PE surfaces. Contact angles (θ) were measured on untreated and HA-treated samples of PS and PE. $\Delta\theta$ presents the difference between the contact angles of the treated and untreated samples. The PS sample had a contact angle of 89.2° which is in accordance with the literature.[78] The PE sample shows more substantial hydrophobic properties with a contact angle of 107.9°, and similar results were found in the literature.[79] Contact angles of both HA-treated PS and PE samples are similar, about 97°. This is most likely a result of the adsorbed HA molecules' similar behaviour on the different microspheres' surfaces. These results indicate that HA forms a similar structure on the treated PS and PE surfaces. Studies of the adsorption of HA on carbonaceous surfaces at

different concentrations of HA showed that HA can form layered structures, which can be considered a supramolecular association.[80] The literature has shown that the adsorption of HA on hydrophobic surfaces such as SiO_2 and polystyrene occurs through hydrophobic interactions.[81,82] It is assumed that before the adsorption, the hydrophobic groups are hidden in the inner part of the HA molecules, so structural rearrangement of the molecule is required.

In addition, the adsorption of HA on the surface of plastic microspheres changes the visual appearance of the microspheres by changing their colour depending on the quantity of adsorbed HA. The colour measurements were performed to determine the HA adsorption on the plastic microspheres (Table 1). The colour properties of the different samples were measured, and the colour change was investigated using CIE colourimetry. A detailed description of the method is given in the ESI.† In the CIELAB system, L^* indicates lightness on a scale from 0 (black) to 100 (white). At the same time, the chromaticity value of a colour is represented in a two-dimensional diagram in which axis a^* determines the ratio of green (negative) to red (positive). Axis b^* determines the blue (negative) to yellow (positive) ratio. ΔE_{ab}^* is the Euclidean distance in CIELAB space, i.e., the colour distance between two colours or the total colour

Table 1 Pellets of untreated and HA-treated polystyrene and poly-ethylene microspheres and their corresponding colour characteristics[a]

	L^*	a^*	b^*	ΔE_{ab}^*	Pellets
PS					
Untreated	97.6	−0.1	−1.2	—	
HA treated	76.9	3.6	5.7	22.1	
PE					
Untreated	94.1	0.6	1.3	—	
HA treated	81.1	3.5	9.3	15.5	

[a] L^* – lightness with a scale from 0 (black) to 100 (white), chromaticity represented in a two-dimensional diagram with axis a^* – the ratio of green (negative) to red (positive) and b^* – the ratio of blue (negative) to yellow (positive). ΔE_{ab}^* is the total colour change or the Euclidean distance in CIELAB space.

change. The results show that both samples of PS and PE were white before treatment, with a^* and b^* values close to 0 and L^* values close to 100. After the adsorption of HA on the surface, changes were observed in $PS(\Delta E_{ab}^* = 22.1)$ and, to a lesser extent, in $PE(\Delta E_{ab}^* = 15.5)$. A value of about 2.3 corresponds to a just noticeable difference.[83] Thus, values of 22 and 15 indicate significant colour changes. In both cases, the adsorption of HA darkens the samples (ΔL^* decreases by 20.6 for PS and 13.0 for PE), *i.e.*, the colour changes from white to light grey. At the same time, it acquires a red hue ($a^* \sim 3.5$) and a much stronger yellow hue ($b^* = 5.7$ for PS and 9.3 for PE), confirming the adsorption of a significant amount of HA on the microplastic surface.

AFM, contact angles, and colour change of the microspheres showed that the surface properties of PS and PE plastic microspheres changed after the treatment with HA, which is also expected in natural aquatic ecosystems. In nature, PS and PE are among the most abundant microplastic particles. In comparison to our model spherical microplastic particles, PS and PE particles in nature are exposed to physical, chemical, and biological processes.[84] Due to these processes, they are fragmented into smaller particles of irregular shape (fragments), and over time the surface roughness of these particles becomes more pronounced.[85–87] Under UV weathering surface oxygen-containing functional groups increase and transform microplastic surface to be more hydrophilic and polar.[88–90] Reduction of surface hydrophobicity, increased charge, and decomposition of the surface structure could all alter interactions between MPs and organic molecules (*e.g.*, hydrophobic, π–π, electrostatic, hydrogen bonding interactions).[91,92] Dissolved organic matter (HA is an active component of DOM) affects interactions between MPs and organic pollutants. Therefore, it is to be

expected that such changes could affect the bioavailability and bioaccumulation of microplastics in natural systems.[93–98] Even though the sampling and characterization of microplastics have recently advanced rapidly, they present significant challenges. They must be improved to evaluate microplastics' presence and consequences in the natural environments.[99]

3.3. Encapsulation of plastic microspheres

SEM and TOC were used to observe the encapsulation of microplastics in aragonite. SEM images of aragonite samples isolated from the reference system and all other systems are shown in Fig. 4 and SI1.† The sample in the reference system consisted of an aragonite polymorph in the form of irregular aggregates with an average size of 3 μm. These crystals showed a typical acicular morphology with elongated needle-like crystals in the *c*-axis direction. They appeared to be radially organized and emerged from a seeding crystallization point. The obtained morphology is similar to other studies performed in artificial seawater,[66,100] in which aragonite was precipitated with the observed characteristic features. The coral skeleton is also built from bundles of acicular aragonite crystals with radial distribution in which aragonite crystals grow in the *c*-axes direction from the centres of calcification.[101,102] Both aragonite from corals and synthetically prepared aragonite exhibit similar crystal orientations and radial growth, making the presented model suitable for researching microplastic encapsulation efficiency in aragonite.

The morphology of aragonite precipitated in the presence of untreated microspheres was not significantly affected. Free PE microspheres and microspheres partially covered with aragonite were observed in these samples. In the sample prepared with HA-treated PE microspheres, free microspheres were hardly detectable due to their more pronounced encapsulation in aragonite. For the samples prepared in the presence of untreated PS microspheres, these microspheres are primarily observed as adsorbed on the surface of the aragonite. In contrast, their partial encapsulation in the aragonite was observed for PS microspheres treated with HA. During crystal growth, the microspheres are overgrown by aragonite (Fig. SI2†), and the SEM images show that the thickness of the aragonite layer around the encapsulated plastic microspheres can be 1.5 μm (Fig. SI3†).

The efficiency of encapsulation of plastic microspheres in aragonite was determined by TOC analysis. As described in the experimental section, the samples were prepared for TOC analysis by dissolving any plastic microspheres that were not encapsulated and completely overgrown by aragonite. This includes dissolving both partially encapsulated/adsorbed and free plastic microspheres, leaving only encapsulated plastic microspheres in aragonite. TOC analysis showed that all types of used microplastics were encapsulated into aragonite. Encapsulation efficiency is presented in Table 2. These results show that more PE than PS was encapsulated, regardless of whether the microplastic particles had been previously treated with HA. Compared to untreated PE, the increase in encapsulation of PE treated with HA was also observed. However, in the

1122 | *Environ. Sci.: Processes Impacts*, 2024, **26**, 1116–1129

This journal is © The Royal Society of Chemistry 2024

Fig. 4 SEM images of aragonite samples in the reference system and the system with untreated and HA-treated PE and PS.

Table 2 Encapsulation efficiency of microplastics (MP) in aragonite: $W_{tot} = m$ (encapsulated MP)$/m$ (initial MP); $W_A = m$ (encapsulated MP)$/m$ (aragonite sample); N – number of encapsulated MP particles in 1 mg of aragonite sample

MP	$W_{tot}/\%$	$W_A/\%$	$N/10^6$
PE	23.6 ± 2.6	0.73 ± 0.08	2.60 ± 0.29
PS	7.2 ± 1.9	0.22 ± 0.06	0.98 ± 0.25
PE-HA	30.7 ± 6.2	0.95 ± 0.19	3.38 ± 0.68
PS-HA	7.4 ± 1.0	0.23 ± 0.03	1.01 ± 0.14

case of PS, there was no significant difference in the amount of encapsulated, treated *versus* untreated PS microparticles.

Although the amounts of encapsulated microplastic particles in aragonite samples (W_A) may appear low, they should not be neglected. Namely, the organic matrix that is, besides $CaCO_3$, a constituent part of biominerals that build hard tissue of marine organisms, is also present in minimal amounts but drastically influences the properties of the associated

biominerals. In coral skeletons, it can be found in amounts less than 0.1% (ref. 103) and mollusc shells up to 5%.[1] When analysed, the fracture toughness of the nacreous layer of the molluscs shell exceeds that of pure inorganic aragonite by two to three orders of magnitude.[104,105] So, the change in aragonite properties due to observed microplastic encapsulation is expected.

The observed enhanced encapsulation of PE treated with HA in aragonite compared to encapsulation of untreated PE is consistent with our previous investigation,[29] in which we showed that adsorption of HA onto PS caused enhanced encapsulation of PS in growing calcite crystals. At the same time, the observed difference between the encapsulation of PS in calcite and the PS in aragonite is interesting as it indicates that polymorphs of calcium carbonate might behave differently in the presence of microplastic particles.

The significant difference in the encapsulation efficiency of PS and PE microspheres raises the question of whether PE microspheres, compared to PS in aquatic ecosystems, will show more pronounced encapsulation into calcium carbonate

This journal is © The Royal Society of Chemistry 2024

Environ. Sci.: Processes Impacts, 2024, **26**, 1116–1129 | **1123**

skeletal structures. It has to be mentioned that in the experiments, the specific surface area of the used untreated PE and PS microspheres (3.86 m^2 g^{-1} for PE and 3.77 m^2 g^{-1} for PS) as well as the size distribution: 1.6 ± 0.2 μm for PS and 1.77 ± 0.48 μm for PE (Fig. SI4†) were very similar, but the surface charge and surface roughness between PS and PE differed significantly. Electrokinetic measurements showed a difference in the zeta potential of PE and PS: −34.4 ± 0.9 mV for PE and −12.8 ± 1.0 mV for PS, indicating that PE was more negatively charged than PS. At the same time, the surface roughness was significantly higher in the case of PE than PS, as determined by AFM measurements. Surface properties such as surface roughness, charge, hydrophilicity, and the presence of functional groups on the surface, affect the precipitation of the mineral phase on that surface. Thus, it is possible to relate the observed difference in the amount of encapsulated PE and PS in aragonite to these two parameters: surface charge and surface roughness.

Calcium ions in solution prefer adsorption to negatively charged surfaces through electrostatic interaction between the ions and the surface.[106] Although contradicting results have been reported on the effect of surface charge on the nucleation of minerals, according to one of the proposed mechanisms,[107] we assume that in our investigated systems, enhanced Ca^{2+} adsorption on the negatively charged surfaces of PE and PS promotes surface nucleation of CaCO$_3$ and subsequent crystal growth of aragonite. Since PE is more negatively charged than PS, more nucleation sites are present on the surface, resulting in aragonite preferentially encapsulating more PE microspheres.

The second parameter that could be related to the encapsulation efficiency is surface roughness. The kinetics of heterogeneous nucleation of mineral phases is known to be enhanced on rough surfaces compared to smooth surfaces.[106,108–110] This could be related to rough surfaces with different convex and concave structures providing a higher surface density of nucleation sites with a reduced activation energy barrier for heterogeneous nucleation. Moreover, the diffusion of constituent ions of precipitating minerals is restrained within the concave structures resulting in localized supersaturation and enhanced surface nucleation. Therefore, CaCO$_3$ crystals preferably nucleate and grow on PE microparticles with higher surface roughness than on PS microparticles, resulting in a higher number of encapsulated PE microparticles.

Encapsulation of PE and PS microspheres might influence the mechanical properties of aragonite, so to further investigate the assumed influence of encapsulation, IIT was carried out. The IIT results presented in Tables 3 and SI2† include indentation modulus (E_{IT}), indentation hardness (H_{IT}), stiffness (S), indentation creep (C_{IT}), and the ratio of elastic work W_{elast} in total work

W_{total} (η_{IT}). As assumed, the carried research showed that encapsulation of treated PS microspheres within the aragonite decreased the E_{IT} and H_{IT} values by approximately 1.4, S by a factor of approximately 1.1, while C_{IT} and η_{IT} are within standard deviation compared to pure aragonite. In contrast, a more prominent decrease in mechanical properties was obtained in the case of aragonite with the encapsulated HA-treated PE. H_{IT} value was decreased by a factor of approx. 1.7, E_{IT} by a factor of approx. 2.7 and S by a factor of approximately 2.0 as compared with pure aragonite. The significant reduction in H_{IT}, E_{IT}, and S coincides with the increase of η_{IT} and C_{IT} during indentation. The decrease in these parameters can be directly attributed to the encapsulated plastic microspheres in aragonite.

PS and PE are, in environmental samples' the most abundant microplastic polymers.[32] Generally, most plastic items in the sea are found to be smaller than 5 mm[111,112] and as irregular fragments.[111,113] As the microplastic size decreases, the potential of bioaccumulation and bioavailability increases.[94] Also, surface roughening indicates microplastic residence time in aquatic environments.[85–87] Therefore, using spherical microplastic particles of PS and PE with uniform size and composition, which are well suited for studying the behaviour of such particles in a complex aquatic environment related to biomineralization, were used in this work.

Conducted research raises concerns regarding the influence of encapsulated plastic on the mechanical properties of skeletal structures of water organisms producing calcium carbonate biominerals. The results show that when compared with pure aragonite, aragonite with the encapsulated microspheres had reduced hardness, elastic/indentation modulus, and stiffness. Similarly, Kim et al. showed that the composite structures of calcite and PS particles had lower stiffness and hardness than the Icelandic spar calcite and sea urchin spine.[28] Recent studies have shown that reef-building corals permanently accumulate up to 2.82% of bioavailable microplastics per year and are considered long-term sinks for microplastics.[26] In aquatic ecosystems, the growth of calcium carbonate skeletal structures in organisms is continuous, and microplastic particles are constantly present, suggesting that the amount of encapsulated microplastics in them may accumulate over time. To date, researchers do not know what effects encapsulated microplastics will have on the stability of coral skeletons.[20,26] As shown in our research, during the application of constant force over 30 seconds, a relative change in indentation depth (C_{IT}) was higher for the PE-HA sample, indicating a lower resistance to time-dependent deformation under constant stress at room temperature. Also, the indentation work ratio (η_{IT}) measured for the PE-HA sample is related to reverse elastic deformation

Table 3 Comparison of indentation modulus (E_{IT}), indentation hardness (H_{IT}), stiffness (S), indentation creep (C_{IT}), and indentation work ratio (η_{IT}) of pure aragonite and samples of aragonite with encapsulated PS-HA and PE-HA microspheres

Sample	E_{IT}/GPa	H_{IT}/MPa	S/mN nm^{-1}	C_{IT}/%	η_{IT}/%
Pure aragonite	31.2 ± 0.4	481.3 ± 16.8	1.74 ± 0.02	5.1 ± 0.3	12.8 ± 0.2
PS-HA	22.6 ± 0.5	336.2 ± 10.5	1.52 ± 0.02	4.9 ± 0.2	12.4 ± 0.2
PE-HA	11.5 ± 1.1	286.1 ± 20.9	0.85 ± 0.11	8.1 ± 0.3	20.0 ± 0.2

1124 | Environ. Sci.: Processes Impacts, 2024, 26, 1116–1129

This journal is © The Royal Society of Chemistry 2024

indicating better ductility for the PE-HA sample. Our research has shown that the encapsulated microplastics have indeed altered the mechanical properties of aragonite, suggesting that more in-depth *in vivo* studies on this subject are needed. Considering that the encapsulation process is complex, it is important to use other methods in future studies, so that, in addition to the efficiency, the encapsulation process and its consequences can be better understood, as well as the possible influence of environmental factors on that process.

4. Conclusion

This novel research demonstrates the encapsulation of PS and PE microspheres in aragonite. The encapsulation efficiency was estimated using the TOC measurement technique after pre-treatment steps to isolate encapsulated microspheres from inorganic/microplastic solid matrix. A much higher encapsulation efficiency of PE compared to PS, both untreated and HA-treated, was observed and could be related to the surface charge and roughness of PE and PS. As determined by AFM measurements, PE had a higher surface roughness than PS in the case of both untreated and HA-treated microplastic particles. These results suggest that the efficiency of encapsulating different types of microplastics in calcium carbonate minerals needs further investigation, both *in vitro* and *in vivo*. As observed by IIT, aragonite with the encapsulated microspheres had reduced hardness, elastic/indentation modulus, stiffness, and lower resistance to time-dependent deformation under constant stress at room temperature. The change in mechanical properties of aragonite after microplastic encapsulation raises concerns about potential skeletal changes that might occur when microplastic particles in aquatic ecosystems become encapsulated in coral skeletal tissue. Our future studies will focus on *in vivo* research in organisms that produce calcium carbonate biominerals to develop conservation strategies and mitigate the effects of microplastics on biomineralized tissues.

Author contributions

Nives Matijaković Mlinarić: funding acquisition, conceptualization, methodology, investigation, formal analysis, visualization, writing – original draft, writing – review & editing; Ivana Stanić: formal analysis; Katarina Marušić: formal analysis; Antun Lovro Brkić: formal analysis; Marijan Marciuš: formal analysis; Tamara Aleksandrov Fabijanić: formal analysis; Nenad Tomašić: formal analysis; Atiđa Selmani: formal analysis, visualization; Eva Roblegg: discussion, writing – review & editing; Damir Kralj: discussion, writing – review & editing; Branka Njegić Džakula: supervision, conceptualization, methodology, visualization, writing – original draft, writing – review & editing; Jasminka Kontrec: funding acquisition, project administration, supervision, conceptualization, methodology, visualization, writing – original draft, writing – review & editing.

Conflicts of interest

There are no conflicts of interest to be declared.

Acknowledgements

References

1 S. Mann, *Biomineralization: Principles and Concepts in Bioinorganic Materials Chemistry*, Oxford University Press on Demand, New York, 2001.

2 P. M. Dove, J. J. De Yoreo and S. Weiner, Biomineralization, *Reviews in Mineralogy and Geochemistry*, Mineralogical Society of America and Geochemical Society, Washington DC, USA, 2003, vol. 54.

3 G. Falini, M. Reggi, S. Fermani, F. Sparla, S. Goffredo, Z. Dubinsky, O. Levi, Y. Dauphin and J.-P. Cuif, Control of aragonite deposition in colonial corals by intra-skeletal macromolecules, *J. Struct. Biol.*, 2013, **183**, 226–238.

4 C. Perdikouri, A. Kasioptas, T. Geisler, B. C. Schmidt and A. Putnis, Experimental study of the aragonite to calcite transition in aqueous solution, *Geochim. Cosmochim. Acta*, 2011, **75**, 6211–6224.

5 M. Boon, W. D. A. Rickard, A. L. Rohl and F. Jones, Stabilization of Aragonite: Role of Mg $^{2+}$ and Other Impurity Ions, *Cryst. Growth Des.*, 2020, **20**, 5006–5017.

6 R. Fisher, R. A. O'Leary, S. Low-Choy, K. Mengersen, N. Knowlton, R. E. Brainard and M. J. Caley, Species richness on coral reefs and the pursuit of convergent global estimates, *Curr. Biol.*, 2015, **25**, 500–505.

7 T. P. Hughes, M. L. Barnes, D. R. Bellwood, J. E. Cinner, G. S. Cumming, J. B. C. Jackson, J. Kleypas, I. A. Van De Leemput, J. M. Lough, T. H. Morrison, S. R. Palumbi, E. H. Van Nes and M. Scheffer, Coral reefs in the Anthropocene, *Nature*, 2017, **546**, 82–90.

8 L. Burke, K. Reytar, M. Spalding and A. Perry, *Reefs at Risk Revisited*, World Resources Institute, Washington DC, 2011, vol. 74.

9 D. P. Häder, A. T. Banaszak, V. E. Villafañe, M. A. Narvarte, R. A. González and E. W. Helbling, Anthropogenic pollution of aquatic ecosystems: Emerging problems with global implications, *Sci. Total Environ.*, 2020, **713**, 136586–136596.

This journal is © The Royal Society of Chemistry 2024

Environ. Sci.: Processes Impacts, 2024, **26**, 1116–1129 | **1125**

10 B. Singh and N. Sharma, Mechanistic implications of plastic degradation, *Polym. Degrad. Stab.*, 2008, **93**, 561–584.

11 OECD, *Global Plastics Outlook: Policy Scenarios to 2060*, OECD Publications, Paris, 2022.

12 L. Lebreton and A. Andrady, Future scenarios of global plastic waste generation and disposal, *Palgrave Commun.*, 2019, **5**, 6.

13 J. R. Jambeck, R. Geyer, C. Wilcox, T. R. Siegler, M. Perryman, A. Andrady, R. Narayan and K. L. Law, Plastic waste inputs from land into the ocean, *Science*, 2015, **347**, 768–771.

14 J. Boucher and D. Friot, *Primary Microplastics in the Oceans: A Global Evaluation of Sources*, IUCN International Union for Conservation of Nature, 2017.

15 United Nations Environment Programme, *From Pollution to Solution: A Global Assessment of Marine Litter and Plastic Pollution. Synthesis*, United Nations Environment Programme (UNEP), Nairobi, 2021.

16 R. Geyer, J. R. Jambeck and K. L. Law, Production, use, and fate of all plastics ever made, *Sci. Adv.*, 2017, **3**, e1700782.

17 W. W. Y. Lau, Y. Shiran, R. M. Bailey, E. Cook, M. R. Stuchtey, J. Koskella, C. A. Velis, L. Godfrey, J. Boucher, M. B. Murphy, R. C. Thompson, E. Jankowska, A. Castillo Castillo, T. D. Pilditch, B. Dixon, L. Koerselman, E. Kosior, E. Favoino, J. Gutberlet, S. Baulch, M. E. Atreya, D. Fischer, K. K. He, M. M. Petit, U. R. Sumaila, E. Neil, M. V. Bernhofen, K. Lawrence and J. E. Palardy, Evaluating scenarios toward zero plastic pollution, *Science*, 2020, **369**, 1455–1461.

18 R. S. Lampitt, S. Fletcher, M. Cole, A. Kloker, S. Krause, F. O'Hara, P. Ryde, M. Saha, A. Voronkova and A. Whyle, Stakeholder alliances are essential to reduce the scourge of plastic pollution, *Nat. Commun.*, 2023, **14**, 2849.

19 G. Birarda, C. Buosi, F. Caridi, M. A. Casu, G. De Giudici, L. Di Bella, D. Medas, C. Meneghini, M. Pierdomenico, A. Sabbatini, A. Surowka and L. Vaccari, Plastics, (bio)polymers and their apparent biogeochemical cycle: An infrared spectroscopy study on foraminifera, *Environ. Pollut.*, 2021, **279**, 116912–116924.

20 F. Hierl, H. C. Wu and H. Westphal, Scleractinian corals incorporate microplastic particles: identification from a laboratory study, *Environ. Sci. Pollut. Res.*, 2021, **28**, 37882–37893.

21 J. Reichert, J. Schellenberg, P. Schubert and T. Wilke, Responses of reef building corals to microplastic exposure, *Environ. Pollut.*, 2018, **237**, 955–960.

22 Z. Han, T. Jiang, L. Xie and R. Zhang, Microplastics impact shell and pearl biomineralization of the pearl oyster Pinctada fucata, *Environ. Pollut.*, 2022, **293**, 118522.

23 C. Martin, E. Corona, G. A. Mahadik and C. M. Duarte, Adhesion to coral surface as a potential sink for marine microplastics, *Environ. Pollut.*, 2019, **255**, 113281.

24 E. Corona, C. Martin, R. Marasco and C. M. Duarte, Passive and Active Removal of Marine Microplastics by a Mushroom Coral (Danafungia scruposa), *Front. Mar. Sci.*, 2020, **7**, 1–9.

25 J. Ding, F. Jiang, J. Li, Z. Wang, C. Sun, Z. Wang, L. Fu, N. X. Ding and C. He, Microplastics in the coral reef systems from Xisha Islands of South China Sea, *Environ. Sci. Technol.*, 2019, **53**, 8036–8046.

26 J. Reichert, A. L. Arnold, N. Hammer, I. B. Miller, M. Rades, P. Schubert, M. Ziegler and T. Wilke, Reef-building corals act as long-term sink for microplastic, *Global Change Biol.*, 2022, **28**, 33–45.

27 G. Mahadevan, Q. Ruifan, Y. H. Hian Jane and S. Valiyaveettil, Effect of Polymer Nano- And Microparticles on Calcium Carbonate Crystallization, *ACS Omega*, 2021, **6**, 20522–20529.

28 Y. Y. Kim, L. Ribeiro, F. Maillot, O. Ward, S. J. Eichhorn and F. C. Meldrum, Bio-inspired synthesis and mechanical properties of calcite-polymer particle composites, *Adv. Mater.*, 2010, **22**, 2082–2086.

29 N. Matijaković Mlinarić, A. Selmani, A. L. Brkić, B. Njegić Džakula, D. Kralj and J. Kontrec, Exposure of microplastics to organic matter in waters enhances microplastic encapsulation into calcium carbonate, *Environ. Chem. Lett.*, 2022, **20**, 2235–2242.

30 J. A. Ivar do Sul, Why it is important to analyze the chemical composition of microplastics in environmental samples, *Mar. Pollut. Bull.*, 2021, **165**, 112086.

31 J. John, A. R. Nandhini, P. Velayudhaperumal Chellam and M. Sillanpää, Microplastics in mangroves and coral reef ecosystems: a review, *Environ. Chem. Lett.*, 2021, 1–20.

32 B. Hufnagl, M. Stibi, H. Martirosyan, U. Wilczek, J. N. Möller, M. G. J. Löder, C. Laforsch and H. Lohninger, Computer-Assisted Analysis of Microplastics in Environmental Samples Based on μFTIR Imaging in Combination with Machine Learning, *Environ. Sci. Technol. Lett.*, 2022, **9**, 90–95.

33 F. Shahul Hamid, M. S. Bhatti, N. Anuar, N. Anuar, P. Mohan and A. Periathamby, Worldwide distribution and abundance of microplastic: How dire is the situation?, *Waste Manage. Res.*, 2018, **36**, 873–897.

34 U. Rozman and G. Kalčíková, Seeking for a perfect (non-spherical) microplastic particle – The most comprehensive review on microplastic laboratory research, *J. Hazard. Mater.*, 2022, **424**, 127529.

35 A. Kundu, N. P. Shetti, S. Basu, K. Raghava Reddy, M. N. Nadagouda and T. M. Aminabhavi, Identification and removal of micro- and nano-plastics: Efficient and cost-effective methods, *Chem. Eng. J.*, 2021, **421**, 129816.

36 A. S. Tagg, M. Sapp, J. P. Harrison and J. J. Ojeda, Identification and Quantification of Microplastics in Wastewater Using Focal Plane Array-Based Reflectance Micro-FT-IR Imaging, *Anal. Chem.*, 2015, **87**, 6032–6040.

37 Z. Sobhani, M. Al Amin, R. Naidu, M. Megharaj and C. Fang, Identification and visualisation of microplastics by Raman mapping, *Anal. Chim. Acta*, 2019, **1077**, 191–199.

38 L. Hermabessiere, C. Himber, B. Boricaud, M. Kazour, R. Amara, A.-L. Cassone, M. Laurentie, I. Paul-Pont, P. Soudant, A. Dehaut and G. Duflos, Optimization, performance, and application of a pyrolysis-GC/MS

1126 | *Environ. Sci.: Processes Impacts*, 2024, **26**, 1116–1129

This journal is © The Royal Society of Chemistry 2024

method for the identification of microplastics, *Anal. Bioanal. Chem.*, 2018, **410**, 6663–6676.

39 E. Dümichen, P. Eisentraut, C. G. Bannick, A.-K. Barthel, R. Senz and U. Braun, Fast identification of microplastics in complex environmental samples by a thermal degradation method, *Chemosphere*, 2017, **174**, 572–584.

40 Y. Hong, J. Oh, I. Lee, C. Fan, S.-Y. Pan, M. Jang, Y.-K. Park and H. Kim, Total-organic-carbon-based quantitative estimation of microplastics in sewage, *Chem. Eng. J.*, 2021, **423**, 130182.

41 C.-S. Chen, C. Le, M.-H. Chiu and W.-C. Chin, The impact of nanoplastics on marine dissolved organic matter assembly, *Sci. Total Environ.*, 2018, **634**, 316–320.

42 H. Luo, Y. Zhao, Y. Li, Y. Xiang, D. He and X. Pan, Aging of microplastics affects their surface properties, thermal decomposition, additives leaching and interactions in simulated fluids, *Sci. Total Environ.*, 2020, **714**, 136862.

43 H. Luo, C. Liu, D. He, J. Xu, J. Sun, J. Li and X. Pan, Environmental behaviors of microplastics in aquatic systems: A systematic review on degradation, adsorption, toxicity and biofilm under aging conditions, *J. Hazard. Mater.*, 2022, **423**, 126915.

44 O. S. Alimi, D. Claveau-Mallet, R. S. Kurusu, M. Lapointe, S. Bayen and N. Tufenkji, Weathering pathways and protocols for environmentally relevant microplastics and nanoplastics: What are we missing?, *J. Hazard. Mater.*, 2022, **423**, 126955.

45 G. Binda, G. Zanetti, A. Bellasi, D. Spanu, G. Boldrocchi, R. Bettinetti, A. Pozzi and L. Nizzetto, Physicochemical and biological ageing processes of (micro)plastics in the environment: a multi-tiered study on polyethylene, *Environ. Sci. Pollut. Res.*, 2023, **30**, 6298–6312.

46 C. Maddison, C. I. Sathish, D. Lakshmi, O. Wayne and T. Palanisami, An advanced analytical approach to assess the long-term degradation of microplastics in the marine environment, *npj Mater. Degrad.*, 2023, **7**, 59.

47 C. M. Rochman, C. Brookson, J. Bikker, N. Djuric, A. Earn, K. Bucci, S. Athey, A. Huntington, H. McIlwraith, K. Munno, H. De Frond, A. Kolomijeca, L. Erdle, J. Grbic, M. Bayoumi, S. B. Borrelle, T. Wu, S. Santoro, L. M. Werbowski, X. Zhu, R. K. Giles, B. M. Hamilton, C. Thaysen, A. Kaura, N. Klasios, L. Ead, J. Kim, C. Sherlock, A. Ho and C. Hung, Rethinking microplastics as a diverse contaminant suite, *Environ. Toxicol. Chem.*, 2019, **38**, 703–711.

48 P. Xu, W. Ge, C. Chai, Y. Zhang, T. Jiang and B. Xia, Sorption of polybrominated diphenyl ethers by microplastics, *Mar. Pollut. Bull.*, 2019, **145**, 260–269.

49 X. Fan, Y. Xie, S. Qian, Y. Xiang, Q. Chen, Y. Yang, J. Liu, J. Zhang and J. Hou, Insights into the characteristics, adsorption and desorption behaviors of microplastics aged with or without fulvic acid, *Environ. Sci. Pollut. Res.*, 2022, **30**, 10484–10494.

50 F. K. Mammo, I. D. Amoah, K. M. Gani, L. Pillay, S. K. Ratha, F. Bux and S. Kumari, Microplastics in the environment: Interactions with microbes and chemical contaminants, *Sci. Total Environ.*, 2020, **743**, 140518.

51 Q. Chen, Q. Wang, C. Zhang, J. Zhang, Z. Dong and Q. Xu, Aging simulation of thin-film plastics in different environments to examine the formation of microplastic, *Water Res.*, 2021, **202**, 117462.

52 J. I. Hedges, Organic matter in sea water, *Nature*, 1987, **330**, 205–206.

53 A. Abdurahman, K. Cui, J. Wu, S. Li, R. Gao, J. Dai, W. Liang and F. Zeng, Adsorption of dissolved organic matter (DOM) on polystyrene microplastics in aquatic environments: Kinetic, isotherm and site energy distribution analysis, *Ecotoxicol. Environ. Saf.*, 2020, **198**, 110658–110664.

54 A. Brewer, I. Dror and B. Berkowitz, The Mobility of Plastic Nanoparticles in Aqueous and Soil Environments: A Critical Review, *ACS ES&T Water*, 2021, **1**, 48–57.

55 V. K. Sharma, X. Ma, B. Guo and K. Zhang, Environmental factors-mediated behavior of microplastics and nanoplastics in water: A review, *Chemosphere*, 2021, **271**, 129597–129605.

56 A. K. Kniggendorf, R. Nogueira, C. Lorey and B. Roth, Calcium carbonate deposits and microbial assemblages on microplastics in oligotrophic freshwaters, *Chemosphere*, 2021, **266**, 128942–128952.

57 Y. Zhang, Y. Luo, X. Yu, D. Huang, X. Guo and L. Zhu, Aging significantly increases the interaction between polystyrene nanoplastic and minerals, *Water Res.*, 2022, **219**, 118544.

58 L. A. Amaral-Zettler, E. R. Zettler, T. J. Mincer, M. A. Klaassen and S. M. Gallager, Biofouling impacts on polyethylene density and sinking in coastal waters: A macro/micro tipping point?, *Water Res.*, 2021, **201**, 117289.

59 S. Zhu, Y. Mo, W. Luo, Z. Xiao, C. Jin and R. Qiu, Aqueous aggregation and deposition kinetics of fresh and carboxyl-modified nanoplastics in the presence of divalent heavy metals, *Water Res.*, 2022, **222**, 118877.

60 S. L. Tracy, D. A. Williams and H. M. Jennings, The growth of calcite spherulites from solution, *J. Cryst. Growth*, 1998, **193**, 382–388.

61 D. Nečas and P. Klapetek, Gwyddion: An open-source software for SPM data analysis, *Cent. Eur. J. Phys.*, 2012, **10**, 181–188.

62 F. A. Andersen and L. Brečević, Infrared spectra of amorphous and crystalline calcium carbonate, *Acta Chem. Scand.*, 1991, **45**, 1018–1024.

63 D. Ren, Q. Feng and X. Bourrat, Effects of Additives and Templates on Calcium Carbonate Mineralization in vitro, *Micron*, 2011, **42**, 228–245.

64 I. Buljan Meić, J. Kontrec, D. Domazet Jurašin, B. Njegić Džakula, L. Štajner, D. M. Lyons, M. Dutour Sikirić and D. Kralj, Comparative Study of Calcium Carbonates and Calcium Phosphates Precipitation in Model Systems Mimicking the Inorganic Environment for Biomineralization, *Cryst. Growth Des.*, 2017, **17**, 1103–1117.

65 S. Fermani, B. Njegić-Džakula, M. Reggi, G. Falini and D. Kralj, Magnesium and temperature control on aragonite crystal aggregation and morphology, *CrystEngComm*, 2017, **19**, 2451–2455.

66 B. Njegić Džakula, S. Fermani, Z. Dubinsky, S. Goffredo, G. Falini and D. Kralj, In Vitro Coral Biomineralization

This journal is © The Royal Society of Chemistry 2024

Environ. Sci.: Processes Impacts, 2024, **26**, 1116–1129 | **1127**

under Relevant Aragonite Supersaturation Conditions, *Chem.–Eur. J.*, 2019, **25**, 10616–10624.

67 J. Fang, Y. Xuan and Q. Li, Preparation of polystyrene spheres in different particle sizes and assembly of the PS colloidal crystals, *Sci. China: Technol. Sci.*, 2010, **53**, 3088–3093.

68 B. C. Smith, The Infrared Spectra of Polymers II: Polyethylene, *Spectroscopy*, 2021, **36**, 24–29.

69 Y. P. Chin, G. Alken and E. O'Loughlin, Molecular Weight, Polydispersity, and Spectroscopic Properties of Aquatic Humic Substances, *Environ. Sci. Technol.*, 1994, **28**, 1853–1858.

70 I. V. Perminova, F. H. Frimmel, A. V. Kudryavtsev, N. A. Kulikova, G. Abbt-Braun, S. Hesse and V. S. Petrosyan, Molecular weight characteristics of humic substances from different environments as determined by size exclusion chromatography and their statistical evaluation, *Environ. Sci. Technol.*, 2003, **37**, 2477–2485.

71 G. Madhu, H. Bhunia, P. K. Bajpai and V. Chaudhary, Mechanical and morphological properties of high density polyethylene and polylactide blends, *J. Polym. Eng.*, 2014, **34**, 813–821.

72 Y. Y. Kim, R. Darkins, A. Broad, A. N. Kulak, M. A. Holden, O. Nahi, S. P. Armes, C. C. Tang, R. F. Thompson, F. Marin, D. M. Duffy and F. C. Meldrum, Hydroxyl-rich macromolecules enable the bio-inspired synthesis of single crystal nanocomposites, *Nat. Commun.*, 2019, **10**, 5682–5697.

73 A. N. Kulak, M. Semsarilar, Y. Y. Kim, J. Ihli, L. A. Fielding, O. Cespedes, S. P. Armes and F. C. Meldrum, One-pot synthesis of an inorganic heterostructure: Uniform occlusion of magnetite nanoparticles within calcite single crystals, *Chem. Sci.*, 2014, **5**, 738–743.

74 B. Pokroy, A. N. Fitch, F. Marin, M. Kapon, N. Adir and E. Zolotoyabko, Anisotropic lattice distortions in biogenic calcite induced by intra-crystalline organic molecules, *J. Struct. Biol.*, 2006, **155**, 96–103.

75 B. Pokroy, A. N. Fitch, P. L. Lee, J. P. Quintana, E. N. Caspi and E. Zolotoyabko, Anisotropic lattice distortions in the mollusk-made aragonite: A widespread phenomenon, *J. Struct. Biol.*, 2006, **153**, 145–150.

76 H. Luo, C. Liu, D. He, J. Sun, A. Zhang, J. Li and X. Pan, Interactions between polypropylene microplastics (PP-MPs) and humic acid influenced by aging of MPs, *Water Res.*, 2022, **222**, 118921.

77 K. N. Fotopoulou and H. K. Karapanagioti, Surface properties of beached plastic pellets, *Mar. Environ. Res.*, 2012, **81**, 70–77.

78 Y. Li, J. Q. Pham, K. P. Johnston and P. F. Green, Contact Angle of Water on Polystyrene Thin Films: Effects of CO_2 Environment and Film Thickness, *Langmuir*, 2007, **23**, 9785–9793.

79 T. K. Glaser, O. Plohl, A. Vesel, U. Ajdnik, N. P. Ulrih, M. K. Hrnčič, U. Bren and L. Fras Zemljič, Functionalization of Polyethylene (PE) and Polypropylene (PP) Material Using Chitosan Nanoparticles with Incorporated Resveratrol as Potential Active Packaging, *Materials*, 2019, **12**, 2118.

80 Z. Liu, Y. Zu, R. Meng, Z. Xing, S. Tan, L. Zhao, T. Sun and Z. Zhou, Adsorption of Humic Acid onto Carbonaceous Surfaces: Atomic Force Microscopy Study, *Microsc. Microanal.*, 2011, **17**, 1015–1021.

81 M. J. Avena and L. K. Koopal, Kinetics of Humic Acid Adsorption at Solid-Water Interfaces, *Environ. Sci. Technol.*, 1999, **33**, 2739–2744.

82 J. Li, S. Ma, X. Li and W. Wei, Adsorption of Tannic Acid and Macromolecular Humic/Fulvic Acid onto Polystyrene Microplastics: A Comparison Study, *Water*, 2022, **14**, 2201.

83 M. Mahy, L. Van Eycken and A. Oosterlinck, Evaluation of Uniform Color Spaces Developed after the Adoption of CIELAB and CIELUV, *Color Res. Appl.*, 1994, **19**, 105–121.

84 H. Yang, G. Chen and J. Wang, Microplastics in the Marine Environment: Sources, Fates, Impacts and Microbial Degradation, *Toxics*, 2021, **9**, 41.

85 B. E. Kanyathare, B. Asamoah, M. U. Ishaq, J. Amoani, J. Räty and K.-E. Peiponen, Identification of Plastic Type and Surface Roughness of Film-Type Plastics in Water Using Kramers–Kronig Analysis, *Chemosensors*, 2020, **8**, 88.

86 T. Bond, J. Morton, Z. Al-Rekabi, D. Cant, S. Davidson and Y. Pei, Surface properties and rising velocities of pristine and weathered plastic pellets, *Environ. Sci.: Processes Impacts*, 2022, **24**, 794–804.

87 K.-E. Peiponen, B. Kanyathare, B. Hrovat, N. Papamatthaiakis, J. Hattuniemi, B. Asamoah, A. Haapala, A. Koistinen and M. Roussey, Sorting microplastics from other materials in water samples by ultra-high-definition imaging, *J. Eur. Opt. Soc.-Rapid*, 2023, **19**, 14.

88 G. Liu, Z. Zhu, Y. Yang, Y. Sun, F. Yu and J. Ma, Sorption behavior and mechanism of hydrophilic organic chemicals to virgin and aged microplastics in freshwater and seawater, *Environ. Pollut.*, 2019, **246**, 26–33.

89 J. Lin, D. Yan, J. Fu, Y. Chen and H. Ou, Ultraviolet-C and vacuum ultraviolet inducing surface degradation of microplastics, *Water Res.*, 2020, **186**, 116360.

90 H. Jiang, J. Bu, K. Bian, J. Su, Z. Wang, H. Sun, H. Wang, Y. Zhang and C. Wang, Surface change of microplastics in aquatic environment and the removal by froth flotation assisted with cationic and anionic surfactants, *Water Res.*, 2023, **233**, 119794.

91 P. Liu, X. Zhan, X. Wu, J. Li, H. Wang and S. Gao, Effect of weathering on environmental behavior of microplastics: Properties, sorption and potential risks, *Chemosphere*, 2020, **242**, 125193.

92 Y. Sun, J. Yuan, T. Zhou, Y. Zhao, F. Yu and J. Ma, Laboratory simulation of microplastics weathering and its adsorption behaviors in an aqueous environment: A systematic review, *Environ. Pollut.*, 2020, **265**, 114864.

93 S. L. Wright, R. C. Thompson and T. S. Galloway, The physical impacts of microplastics on marine organisms: a review, *Environ. Pollut.*, 2013, **178**, 483–492.

1128 | *Environ. Sci.: Processes Impacts*, 2024, **26**, 1116–1129

This journal is © The Royal Society of Chemistry 2024

94 S. L. Wright, D. Rowe, R. C. Thompson and T. S. Galloway, Microplastic ingestion decreases energy reserves in marine worms, *Curr. Biol.*, 2013, **23**, R1031–R1033.

95 J. E. Ward and D. J. Kach, Marine aggregates facilitate ingestion of nanoparticles by suspension-feeding bivalves, *Mar. Environ. Res.*, 2009, **68**, 137–142.

96 E. Besseling, J. T. K. Quik, M. Sun and A. A. Koelmans, Fate of nano- and microplastic in freshwater systems: A modeling study, *Environ. Pollut.*, 2017, **220**, 540–548.

97 J. R. Bermúdez, M. Metian, F. Oberhänsli, A. Taylor and P. W. Swarzenski, Preferential grazing and repackaging of small polyethylene microplastic particles ($\leq$ 5 μm) by the ciliate Sterkiella sp, *Mar. Environ. Res.*, 2021, **166**, 105260.

98 C. Scherer, N. Brennholt, G. Reifferscheid and M. Wagner, Feeding type and development drive the ingestion of microplastics by freshwater invertebrates, *Sci. Rep.*, 2017, **7**, 17006.

99 *Oceanography and Marine Biology*, ed. S. J. Hawkins, A. L. Allcock, A. E. Bates, A. J. Evans, L. B. Firth, C. D. McQuaid, B. D. Russell, I. P. Smith, S. E. Swearer and P. A. Todd, CRC Press, 2020.

100 B. Njegić-Džakula, M. Reggi, G. Falini, I. Weber, L. Brečević and D. Kralj, The influence of a protein fragment extracted from abalone shell green layer on the precipitation of calcium carbonate polymorphs in aqueous media, *Croat. Chem. Acta*, 2013, **86**, 39–47.

101 M. Sugiura, K. Yasumoto, M. Iijima, Y. Oaki and H. Imai, Morphological study of fibrous aragonite in the skeletal framework of a stony coral, *CrystEngComm*, 2021, **23**, 3693–3700.

102 C. Y. Sun, M. A. Marcus, M. J. Frazier, A. J. Giuffre, T. Mass and P. U. P. A. Gilbert, Spherulitic Growth of Coral Skeletons and Synthetic Aragonite: Nature's Three-Dimensional Printing, *ACS Nano*, 2017, **11**, 6612–6622.

103 B. Constantz and S. Weiner, Acidic macromolecules associated with the mineral phase of scleractinian coral skeletons, *J. Exp. Zool.*, 1988, **248**, 253–258.

104 J. D. Taylor and M. Layman, The mechanical properties of bivalve (Mollusca) shell structures, *Palaeontology*, 1972, **15**, 73–87.

105 A. P. Jackson, J. F. V. Vincent and R. M. Turner, Comparison of nacre with other ceramic composites, *J. Mater. Sci.*, 1990, **25**, 3173–3178.

106 J. Rolf, T. Cao, X. Huang, C. Boo, Q. Li and M. Elimelech, Inorganic Scaling in Membrane Desalination: Models, Mechanisms, and Characterization Methods, *Environ. Sci. Technol.*, 2022, **56**, 7484–7511.

107 H. Deng, X.-M. Wang, C. Du, X.-C. Shen and F.-Z. Cui, Combined effect of ion concentration and functional groups on surface chemistry modulated $CaCO_3$ crystallization, *CrystEngComm*, 2012, **14**, 6647.

108 M. Qian and J. Ma, The characteristics of heterogeneous nucleation on concave surfaces and implications for directed nucleation or surface activity by surface nanopatterning, *J. Cryst. Growth*, 2012, **355**, 73–77.

109 W. C. Cheong, P. H. Gaskell and A. Neville, Substrate effect on surface adhesion/crystallisation of calcium carbonate, *J. Cryst. Growth*, 2013, **363**, 7–21.

110 N. H. Lin and Y. Cohen, QCM study of mineral surface crystallization on aromatic polyamide membrane surfaces, *J. Membr. Sci.*, 2011, **379**, 426–433.

111 A. Marrone, M. F. La Russa, L. Randazzo, D. La Russa, E. Cellini and D. Pellegrino, Microplastics in the Center of Mediterranean: Comparison of the Two Calabrian Coasts and Distribution from Coastal Areas to the Open Sea, *Int. J. Environ. Res. Public Health*, 2021, **18**, 10712.

112 M. Eriksen, L. C. M. Lebreton, H. S. Carson, M. Thiel, C. J. Moore, J. C. Borerro, F. Galgani, P. G. Ryan and J. Reisser, Plastic Pollution in the World's Oceans: More than 5 Trillion Plastic Pieces Weighing over 250,000 Tons Afloat at Sea, *PLoS One*, 2014, **9**, e111913.

113 S. Morét-Ferguson, K. L. Law, G. Proskurowski, E. K. Murphy, E. E. Peacock and C. M. Reddy, The size, mass, and composition of plastic debris in the western North Atlantic Ocean, *Mar. Pollut. Bull.*, 2010, **60**, 1873–1878.

This journal is © The Royal Society of Chemistry 2024

Environ. Sci.: Processes Impacts, 2024, **26**, 1116–1129 | 1129